第 30 卷第 9 期
2014 年 9 月

无 机 化 学 学 报
CHINESE JOURNAL OF INORGANIC CHEMISTRY

Vol.30 No.9
2127-2133

基于四溴代对苯二甲酸构筑的两个 Cu(Ⅱ) 配位聚合物的合成与晶体结构

肖立群　乔晋忠　胡拖平*

(中北大学理学院,化学系,太原　030051)

摘要：在室温条件下,以甲醇和水为混合溶剂,由四溴代对苯二甲酸(H_2TBTA)和硝酸铜分别与吡啶(py)和咪唑(im)构筑了 2 个一维(1D)铜配位聚合物:$[Cu(TBTA)(py)_3]_n$ (**1**)和$\{[Cu(TBTA)(im)_3]\cdot(H_2O)\}_n$ (**2**),对 2 个配合物进行了元素分析、红外分析、热重分析和 X-射线单晶衍射等表征。在配合物 **1** 和 **2** 中,中心 Cu(Ⅱ)离子都处于五配位环境;H_2TBTA 配体中羧基均采用单齿配位模式;配合物 **2** 存在 π-π 相互作用且氢键较 **1** 丰富。

关键词：铜配合物；四溴代对苯二甲酸；氢键；π-π 作用

中图分类号：O614.121　　**文献标识码**：A　　**文章编号**：1001-4861(2014)09-2127-07

DOI:10.11862/CJIC.2014.267

Syntheses and Crystal Structures of Two Cu(Ⅱ) Coordination Complexes Based on 2,3,5,6-Tetrabromoterephthalic Acid

XIAO Li-Qun　QIAO Jin-Zhong　HU Tuo-Ping*

(*Department of Chemistry, College of Science, North University of China, Taiyuan* 030051, *China*)

Abstract: Two one dimension (1D) Cu(Ⅱ) complexes with 2,3,5,6-tetrabromoterephthalic acid (H_2TBTA), $[Cu(TBTA)(py)_3]_n$ (**1**) (py=pyridine) and $\{[Cu(TBTA)(im)_3]\cdot(H_2O)\}_n$ (**2**) (im=imdazole) were synthesized in CH_3OH/H_2O mixed solution at room temperature, which have been characterized by element analyses, IR spectra, thermogravimetric analyses and single-crystal X-ray diffraction. In complexes **1** and **2**, each center Cu(Ⅱ) ion is five-coordinated and all carboxylate groups of H_2TBTA adopt mono-dentate coordination mode. H-bonding interactions in complex **2** are richer than **1** and there exists π-π interactions in **2**. CCDC: 946787, **1**; 911736, **2**.

Key words: Cu(Ⅱ) complex; 2,3,5,6-tetrabromoterephthalic acid; H-bonding; π-π interaction

0 Introduction

The rich ongoing research of the design and synthesis of metal-organic frameworks (MOFs) and their potential applications such as catalyses, separation, gas storage, optoelectronics, chemical sensors and membranes[1-7] is a testament that lively interest has been evoked in supramolecule chemistry and crystal engineer of MOFs[8-10]. As we known, benzenecarboxylates ligands have made vital contribution to the structural and functional versatility of MOFs[11]. As a kind of benzenecarboxylic ligands, 2,3,5,6-tetrabromoterephthalic acid (H_2TBTA) has been less well studied because of the increasing of steric hindrance effect caused by four Br substituents[12]. But to construct novel MOFs, we should also take certain factors into

收稿日期:2013-08-14。收修改稿日期:2014-04-02。

国家国际科技合作(No.2011DFA51980)和省自然科学基金(No.2011081022)资助项目。

*通讯联系人。E-mail:hutuopingsx@126.com

account, such as the coordination nature of the metal ions and functionality, flexibility and symmetry of ligands as well as the unique reaction methods [13]. Based on the strong coordination ability and the rich coordination modes of carboxylate groups from H_2TBTA, the employment of secondary organic ligands and judicious choice of the central metals become an effective approach to obtain novel topologies. So some complexes (1D or 2D) based on H_2TBTA have been reported by rational choice of the secondary N-donor ligands (such as 1,10-phenanthroline, 2,2′-bipyridine, 4,4′-bipyridine and 1,3-bis(4-pyridyl)propane)[14-19]. As N-donors, pyridine (py) and imidazole (im) are good ligands to design and construct low-dimensional MOFs due to their coordination nature. Different from py, every im molecule possesses two N atoms in different environments which may provide more roles in constructing MOFs and increase the H-bonding interactions. Meanwhile, non-covalent interactions between infinite chains can lead to the formation of interesting architectures[20]. In this thesis, we carried the study of the complexes based on the mixed ligands of H_2TBTA and N-donors (py and im) in CH_3OH/H_2O mixed solution at room temperature.

1 Experimental

1.1 Materials and methods

All reagents and solvents employed were commercially available and used as received. The structures of the complexes **1** and **2** were determined on a Bruker Apex Ⅱ CCD diffractometer and a SuperNova diffractometer equipped with an Atlas CCD detector respectively and solved by direct methods using the SHELXTL program. Elemental analyses were performed by a Vario EL analyzer. The IR spectra on KBr pellets were recorded on a FTIR-8400S spectrometer in the range 4 000~400 cm^{-1}. The thermogravimetric analyses were conducted on a ZCT-A analyzer at the heating rate of 10 ℃·min^{-1} under air atmosphere.

1.2 Synthesis of $[Cu(TBTA)(py)_3]_n$ (1)

A distilled water solution (5 mL) of H_2TBTA (10 mg, 0.02 mol) adjusted to pH=6~7 with py was placed at the bottom of a straight glass tube, then a CH_3OH solution (5 mL) containing $Cu(NO_3)_2·3H_2O$ (20 mg, 0.083 mmol) was carefully laid onto it. The tube was sealed and stood at room temperature. Blue block crystal suitable for XRD was produced after 3 d in 55% yield. Anal. Calcd. (%) for $C_{23}H_{15}Br_4N_3O_4Cu$ (780.56): C 35.39, H 1.94, N 5.38. Found (%): C 34.82, H 1.87, N 5.54. IR (KBr, cm^{-1}): 1 604 (vs), 1 388 (s), 1 227 (w), 1 079 (m), 829 (w), 701 (m), 567 (w).

1.3 Synthesis of $\{[Cu(TBTA)(im)_3]·(H_2O)\}_n$ (2)

A distilled water solution (5 mL) containing H_2TBTA (10 mg, 0.02 mol) and im (4 mg, 0.06 mmol) was placed at the bottom of a straight glass tube, upon which a solution of $Cu(NO_3)_2·3H_2O$ (15 mg, 0.06 mmol) in CH_3OH (5 mL) was carefully laid. The tube was sealed and stood at room temperature. Blue block crystal suitable for XRD was produced after 7 d in 60% yield. Anal. Calcd. for (%) $C_{17}H_{14}N_6O_5Br_4Cu$ (765.52): C 26.65, H 1.83, N 10.97. Found (%): C 26.53, H 1.79, N 10.81. IR (KBr, cm^{-1}): 3 414 (m), 1 618 (vs), 1 536 (m), 1 408 (m), 1 326 (s), 1 080 (m), 834 (m), 779 (w), 578 (w).

1.4 X-ray data collection and structure refinement

Data collection for complex **1** (size: 0.18 mm×0.15 mm×0.10 mm) was performed on a Bruker Smart APEX Ⅱ CCD diffractometer at 273 K by using a graphite-monothematic Mo $K\alpha$ radiation (λ=0.071 073 nm) and complex **2** (size: 0.15 mm×0.20 mm×0.15 mm) was collected on a SuperNova diffractometer equipped with a copper micro-focus X-ray sources (λ= 0.154 06 nm) at 292.39(13) K. Structural solutions were performed by direct method using SHELXS-97[21] program and structures were refined by full-matrix least squares techniques with SHELXL-97[22]. All non-hydrogen atoms were placed in successive difference Fourier syntheses and refined with anisotropic thermal parameters on F^2. The organic hydrogen atoms were geometrically generated and refined by a riding mode. Main crystallographic data and refinements for complexes are given in Table 1 and selected bond lengths and angles are summarized in Table 2.

CCDC: 946787, **1**; 911736, **2**.

Table 1　Crystal data and structure refinement for complexes 1 and 2

Complex	**1**	**2**
Empirical formula	$C_{23}H_{15}Br_4N_3O_4Cu$	$C_{17}H_{14}N_6O_5Br_4Cu$
Formula weight	780.56	765.52
Temperature / K	273.0	292.39(13)
Crystal system	Monoclinic	Triclinic
Space group	*C*2/*c*	$P\bar{1}$
a / nm	1.556 1(3)	0.907 76(7)
b / nm	0.920 49(19)	0.917 53(7)
c / nm	1.832 2(4)	1.410 81(9)
α / (°)		75.809(6)
β / (°)	109.001(3)	86.857(6)
γ / (°)		81.134(6)
Volume / nm	2.481 5(9)	1.125 41(14)
Z	4	2
D_c / (g·cm^{-3})	2.089	2.259
μ / mm^{-1}	7.357	10.088
F(000)	1 500.0	734.0
Crystal size / mm	0.18×0.15×0.10	0.15×0.20×0.15
2θ range for data collection / (°)	4.7 to 55.46	3.232 to 66.6
Index ranges	$-20 \leqslant h \leqslant 20, -8 \leqslant k \leqslant 12, -22 \leqslant l \leqslant 22$	$-10 \leqslant h \leqslant 9, -10 \leqslant k \leqslant 10, -16 \leqslant l \leqslant 12$
Reflections collected	7 214	7 199
Independent reflections	2 852 (R_{int}=0.025 8)	3 950 (R_{int}=0.019 3)
Data / restraints / parameters	2 852 / 0 / 160	3 950 / 0 / 234
Goodness-of-fit on F^2	1.074	1.082
Final *R* indexes ($I>2\sigma(I)$)	R_1=0.049 9, wR_2=0.152 3	R_1=0.023 9, wR_2=0.060 0
Final *R* indexes (all data)	R_1=0.067 8, wR_2=0.164 5	R_1=0.025 9, wR_2=0.061 0
Largest diff. peak, hole / (e·nm^{-3})	3 180, −1 140	390, −530

Table 2　Selected bond lengths (nm) and bond angles (°) for complexes 1 and 2

		1			
Cu(1)-N(1)a	0.200 4(5)	Cu(1)-N(2)	0.205 8(6)	Cu(1)-O(2)	0.211 8(4)
Cu(1)-N(1)	0.200 4(5)	Cu(1)-O(2)a	0.211 8(4)		
N(1)a-Cu(1)-N(1)	177.0(2)	N(1)a-Cu(1)-O(1)	93.19(17)	N(1)-Cu(1)-O(2)a	93.19(17)
N(1)-Cu(1)-N(2)	91.48(12)	N(1)-Cu(1)-O(2)	84.87(16)	N(2)-Cu(1)-O(2)	130.73(11)
N(1)a-Cu(1)-N(2)	91.48(12)	N(1)a-Cu(1)-O(2)	84.87(16)	N(2)-Cu(1)-O(2)a	130.73(11)
O(2)a-Cu(1)-O(2)	98.5(2)				
		2			
Cu(1)-N(3)	0.197 77	Cu(1)-O(3)	0.210 63(18)	Cu(1)-N(1)	0.195 43
Cu(1)-N(5)	0.205 92	Cu(1)-O(1)	0.222 5(2)		
O(3)-Cu(1)-O(1)	117.60(9)	N(1)-Cu(1)-N(5)	93.0	N(3)-Cu(1)-N(5)	92.7
N(1)-Cu(1)-O(3)	88.08(5)	N(3)-Cu(1)-O(3)	88.70(6)	N(5)-Cu(1)-O(3)	136.62(6)
N(1)-Cu(1)-O(1)	89.63(6)	N(3)-Cu(1)-O(1)	87.56(6)	N(5)-Cu(1)-O(3)	105.77(8)
N(1)-Cu(1)-N(3)	174.2				

Symmetry code: a: 1−*x*, *y*, 1/2−*z*

2 Results and discussion

2.1 IR spectrum

In the IR spectrums of complex **1**, there is no characteristic band at 3 300 cm^{-1} means no water molecule exists while the broad peak at 3 414 cm^{-1} belongs to free water molecule in **2**. The asymmetric stretching vibration ($\nu_{as}(COO^-)$) and symmetric stretching vibration ($\nu_s(COO^-)$) of carboxylate groups appear at 1 604, 1 388 and 1 618, 1 408 cm^{-1}, respectively. The $\Delta\nu(\Delta\nu=\nu_{as}(COO^-)-\nu_s(COO^-))$ are 216 cm^{-1} (>200 cm^{-1}) in **1** and 218 cm^{-1} (>200 cm^{-1}) in **2**. These values indicate the carboxylate groups coordinated in monodentated mode[23]. The peak at 1 227 cm^{-1} assigns to the stretching vibration of -N=C- from py ligand in **1**. Similarly, The peak of the stretching vibration of -N=C- from im ligand appears at 1 563 cm^{-1}.

2.2 Crystal structrues of complexes

2.2.1 $[Cu(TBTA)(Py)_3]_n$ (**1**)

Complex **1** crystallizes in the monoclinic system with *C*2/*c* space group. As shown in Fig.1, each Cu(Ⅱ) ion is five-coordinated by two oxygen atoms from two $TBTA^{2-}$ anions, respectively, three nitrogen atoms from three pyridine molecule and has distorted trigonal bipyramid coordination geometry. Its equatorial plane is occupied by three nitrogen atoms, N(1), N(2), N(1)a, and axial position is occupied by two oxygen atoms (Cu(1)-N(1)a 0.200 4(5) nm; Cu(1)-N(1) 0.200 4(5) nm; Cu(1)-N(2) 0.205 8(6) nm; Cu(1)-O(2) 0.211 8(4) nm; Cu(1)-O(2)a 0.211 8(4) nm). The bond distances are in the normal range. The bond angle of O(2)a-Cu(1)-O(2) is 98.5(2)°. The sum of the bond angles of N(1)a-Cu(1)-N(1), N(1)-Cu(1)-N(2) and N(1)a-Cu(1)-N (2) is 359.98°.The uncoordinated oxygen atoms of H_2TBTA ligands act as acceptors to form strong H-bonding interactions with hydrogen atoms provided by py ligands (Fig.2). The data of H-bonding interactions which play an important role in stabilizing the structure are listed in Table 3 in detail.

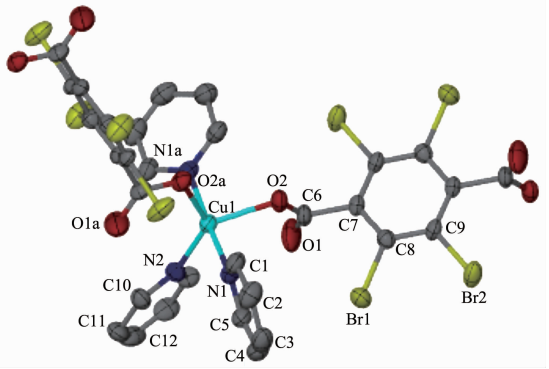

All H atoms are omitted for clarity; Symmetry code: a: 1−*x*, *y*, 1/2−*z*

Fig.1 Coordination environment of complex **1** with thermal ellipsoids at 50% probability

Table 3 Hydrogen bond lengths and bond angles for complexes 1 and 2

D−H···A	*d*(D-H) / nm	*d*(H···A) / nm	*d*(D···A) / nm	∠DHA / (°)
1				
C(1)−H(1)···O(2)a	0.093	0.236	0.296 1(8)	122
C(1)−H(1)···Br(2)b	0.093	0.289	0.350 3(7)	125
C(10)−H(10)···O(1)a	0.093	0.253	0.323 2(7)	132
2				
O(5)−H(5A)···O(3)	0.085	0.202	0.281 7(2)	157
N(2)−H(2)···O(5)c	0.088	0.192	0.279 45(11)	174
N(4)−H(4)···O(2)d	0.088	0.204	0.284 0(2)	150
O(5)−H(5B)···O(2)e	0.075	0.204	0.274 9(2)	158
N(6)−H(6)···O(4)f	0.088	0.204	0.280 7(2)	146
C(13)−H(13)···O(5)g	0.095	0.256	0.336 59(12)	142
C(16)−H(16)···O(5)h	0.095	0.247	0.334 46(12)	154
C(7)−H(7)···O(3)	0.095	0.257	0.296 6(2)	106
C(15)−H(15)···O(4)	0.095	0.232	0.307 5(2)	136

Symmetry codes: **1**: a: 1−*x*, *y*, 1/2−*z*; b: *x*−1/2, 1/2−*y*, *z*−1/2; **2**: c: *x*, 1+*y*, *z*; d: −*x*, −*y*, 1−*z*; e: 1−*x*, −*y*, 1−*z*; f: −*x*, 1−*y*, −*z*; g: −1+*x*, *y*, *z*; h: −1+*x*, 1+*y*, *z*.

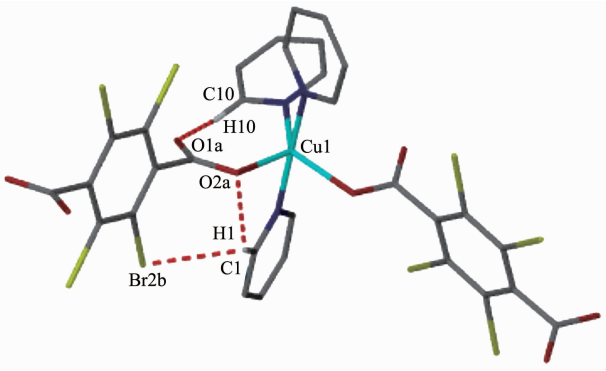

Irrelative H atoms are omitted for clarity; Symmetry codes: a: 1−*x*, *y*, 1/2−*z*; b: *x*−1/2, 1/2−*y*, *z*−1/2

Fig.2　Intramolecular H-bonding interactions of complex **1** (dashed lines)

In complex **1**, both carboxylate groups of H_2TBTA ligands are deprotonated and adopt mono-dentate mode. Py molecules coordinated as end ligands. The adjacent Cu cations are connected by $TBTA^{2-}$ in trans mode to extend to be a 1D chain (Cu⋯Cu 1.132 5 nm) (Fig.3).

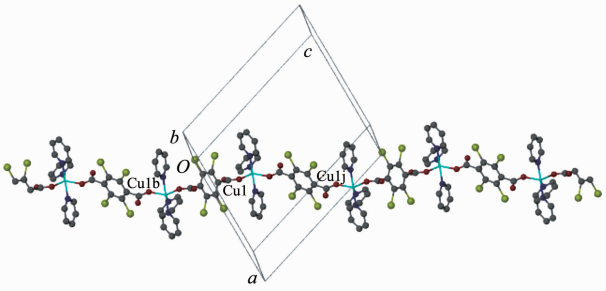

All H atoms are omitted for clarity; Symmetry codes: b: *x*−1/2, 1/2−*y*, *z*−1/2; j: 3/2−*x*, 1/2−*y*, 1−*z*

Fig.3　1D polymeric chain of complex **1**

2.2.2　{[Cu(TBTA)(im)$_3$]·(H_2O)}$_n$ (**2**)

Complex **2** crystallizes in the triclinic system with $P\bar{1}$ space group. As shown in Fig.4, the coordination environment and structure of **2** is similar to **1**, except for py replaced by im, which acted as the end ligands and a free H_2O molecule present in **2**. It is interesting to find that using im instead of py lead to richer hydrogen bonds and a part of H-bonding interactions stabilize the free H_2O molecules (Fig.5), and there exist π-π interactions between im and benzene

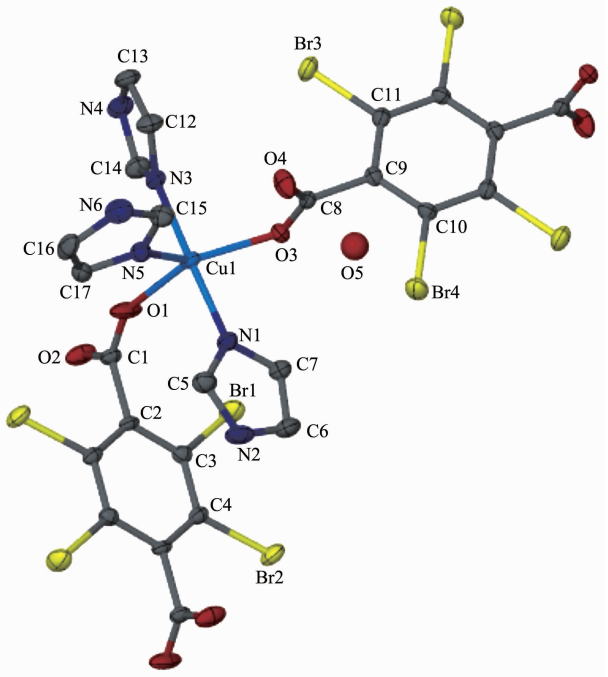

All H atoms are omitted for clarity

Fig.4　Coordination environment of complex **2** with thermal ellipsoids at 50% probability

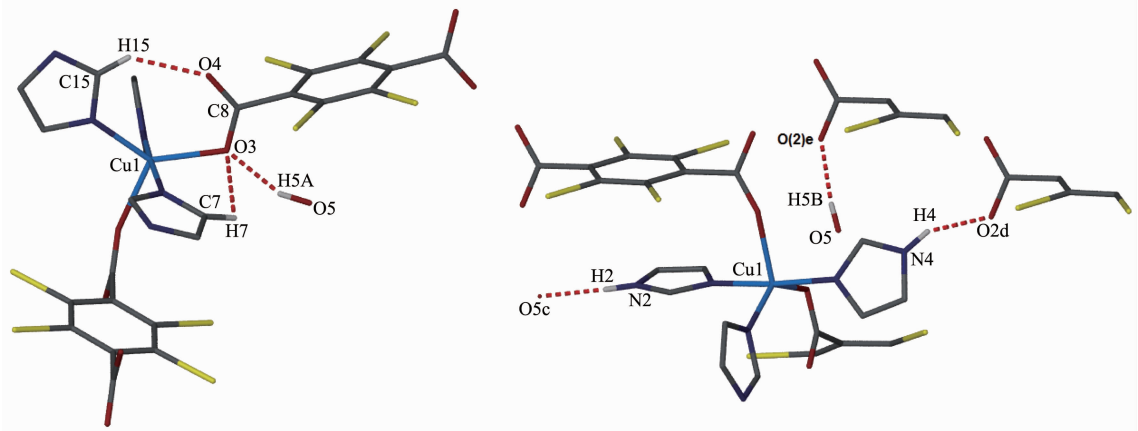

Irrelative H atoms are omitted for clarity; Symmetry codes: c: *x*, 1+*y*, *z*; d: −*x*, −*y*, 1−*z*; e: 1−*x*, −*y*, 1−*z*

Fig.5　(a) Intramolecular H-bonding interactions of complex **2** (dashed lines); (b) Intermolecular H-bonding interactions of complex **2** (dashed lines)

ring from $TBTA^{2-}$. The dihedral angle is 1.696° and the distance of Cg(1)…Cg(2) is 0.351 61(7) nm (Cg(1) is the ring centroid of N(1)-C(5)-N(2)-C(6)-C(7), Cg(2) is the ring centroid of C(2)-C(3)-C(4)-C(2)c-C(3)c-C(4)c). Then the 1D chain of complex **2** is also extended by $TBTA^{2-}$ in mono-dentate mode (Cu(1)…Cu(1)k 1.1277 nm; Cu(1)…Cu(1)i 0.998 2 nm) (Fig.7).

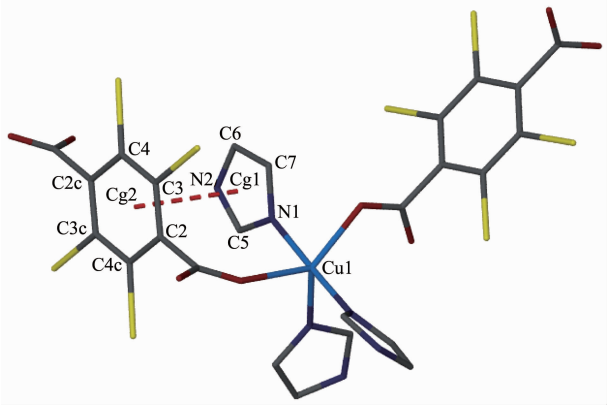

All H atoms are omitted for clarity; Symmetry code: c: 1–x, 2–y, –z

Fig.6 π-π interactions of complex **2**

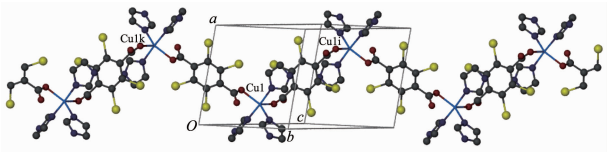

All H atoms are omitted for clarity; Symmetry codes: i: 1–x, 1–y, 1–z; k: 1–x, –y, –z

Fig.7 1D chain of complex **2**

2.3 Thermogravimetric analyses

Thermogravimetric analyses were performed in air from room temperature to 800 ℃. The TG curve of complex **1** shows two steps of weight losses and it is stability before 189 ℃ (Fig.8). The first weight loss is 56.52% from 189 to 439 ℃ corresponds to the remove of $TBTA^{2-}$ ions (Calcd. 61.46%). The second is 31.63% from 439 to 586 ℃ dues to the release of py ligands. Then following a plateau reveals no weight loss after 586 ℃ and the resulting residue is CuO (Obsd. 11.57%; Calcd. 10.19%).

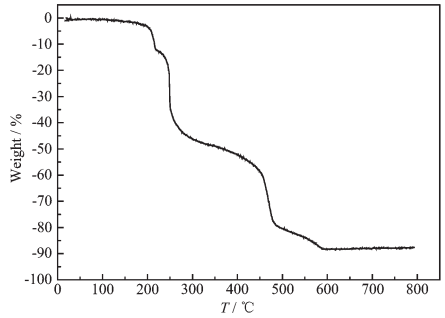

Fig.8 Thermal analysis curve of complex **1**

In complex **2** (Fig.9), the TG curve exhibits that it is stable up to 142 ℃ and an initial weight loss of 3.37% from 142 to 168 ℃ due to the remove of guest water molecules (Calcd. 2.35%). Then an obvious weight loss (60.03%) occurs from 168 to 469 ℃ belongs to the remove of $TBTA^{2-}$ ions (Calcd. 62.66%). The weight loss of 25.45% from 469 to 708 ℃ corresponds to the release of im ligands (Calcd. 26.65%). The residual weight is CuO (Obsd. 8.17%, Calcd. 10.45%). The results indicate that complex **2** is more stable than **1**, maybe due to the richer H-bonding interactions and π-π interactions.

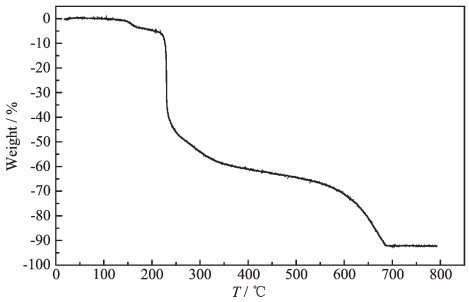

Fig.9 Thermal analysis curve of complex **2**

Reference:

[1] Uraguchi D, Ueki Y, Ooi T. *Science*, **2009**,**326**:120-123

[2] Pan L, Sander M B, Huang X, et al. *J. Am. Chem. Soc.*, **2004**,**126**(5):1308-1309

[3] Kondo M, Yoshitomi T, Seki K, et al. *Angew. Chem. Int. Ed. Engl.*, **1997**,**36**:1725-1727

[4] Reineke T M, Eddaoudi M, O′Keefe M, et al. *Angew. Chem. Int. Ed.*, **1999**,**38**:2590-2594

[5] Holman K T, Pivovar A M, Ward M D. *Science*, **2001**,**294**: 1907-1911

[6] Lee S J, Lin W. *Acc. Chem. Res.*, **2008**,**41**(4):521-537

[7] Gascon J, Kapteijn F. *Angew. Chem., Int. Ed.*, **2010**,**49**:1530 -1532

[8] Zhao D, Timmons D J, Yuan D, et al. *Acc. Chem. Res.*, **2011**, **44**:123-133

[9] Tranchemontagne D J, Mendoza-Cortes J L, O′Keeffe M, et al. *Chem. Soc. Rev.*, **2009**,**38**:1257-1283

[10]Robson R. *J. Chem. Soc. Dalton Trans.*, **2000**,**21**:3735-3744

[11]Cook T R, Zheng Y R, Stang P J. *Chem. Rev.*, **2013**,**113**(1):

734-777

[12]JIN Mei-Fang(靳梅芳). *Thesis for the Master of Shandong University*(山东大学硕士论文). **2010**.

[13]Braga D, Maini L, Polito M, et al. *Coord. Chem. Rev.*, **2003**, **246**:53-71

[14]LIU Yan(刘艳), GAO Ling-Ling(高玲玲), LÜ Xu-Yan (吕旭燕), et al. *Chinese J. Inorg. Chem.*(无机化学学报), **2011**, **28**(8):1623-1628

[15]LIU Jian-Feng(刘建锋), LIU Yan(刘艳), LÜ Xu-Yan (吕旭燕), et al. *Chinese J. Inorg. Chem.*(无机化学学报), **2013**, **29**(1):155-159

[16]LÜ Xu-Yan(吕旭燕), LIU Jian-Feng(刘建锋), LIU Yan(刘艳), et al. *Chinese J. Inorg. Chem.*(无机化学学报), **2013**,**29**(5):1096-1102

[17]Wang X L, Bi Y F, Lin H Y, et al. *Cryst. Growth Des.*, **2007**,**7**:1086-1091

[18]Wang X L, Qin C, Wang E B, et al. *Angew. Chem., Int. Ed.*, **2005**,**44**:5824-5827

[19]Gomez-Lor B, Gutierrez-Puebla E, Iglesias M, et al. *Chem. Mater.*, **2005**,**17**:2568-2573

[20]Leong W L, Vittal J J. *Chem. Rev.*, **2011**,**111**:688-764

[21]Sheldrick G M. *SHELXS*97, *Program for the Solution of Crystal Structure Solution*, Germany, University of Göttingen, **1997**.

[22]Sheldrick G M. *SHELXL*97, *Program for the Solution of Crystal Structure Refinement*, Germany, University of Göttingen, **1997**.

[23]Nakamoto K. *Infrared and Raman Spectra of Inorganic and Coordination Compounds*. *5th Ed*. New York: Wiley Interscience, **1997**.